ORIGINAL PAPER

In vitro release study of electrospun poly(ε-caprolactone)/ gelatin nanofiber mats loaded with 5-fluorouracil

Moshera Samy[1] [ORCID] **· Basma Ekram**[1] **· Bothaina M. Abd El-Hady**[1] **· Magdy M. H. Ayoub**[1]

© The Author(s) 2023

Abstract

The electrospinning process was used to successfully encapsulate an anticancer drug, 5-fluorouracil (5-FU), into poly(ε-caprolactone)/gelatin (Gel) nanofiber mats (5-FU-PCL/Gel NFs). Nanofibers are recognized to be potential carriers for the delivery of anticancer drugs. One of the safest solvent systems for making PCL/ Gel NF mats is the formic acid/acetic acid (FA/AA) solvent system. A compound solution jet was drawn from a customized coaxial spinneret using a high potential electric field of 20 kV. The loading of 5-FU with three different concentrations (5, 10, and 15 wt.%) improved PCL stabilization in the FA/AA system. The miscibility of the blended polymers in the electrospun nanofibers mats and 5-FU being well distributed in the nanofiber matrix was investigated using X-ray diffraction (XRD). In vitro 5-FU release from electrospun PCL/Gel NF mats revealed sustained release from the nanofiber mats, whereas slower release was found when higher concentrations of 5-FU were used. The produced electrospun PCL/Gel NF mats were studied by SEM, FTIR, TGA, and DSC. According to a study on drug release kinetics, 5-FU was released from PCl/Gel NFs in a diffusion-controlled pattern.

Keywords Electrospinning · 5-Fluorouracil · PCL · Gelatin · Nanofibers · Drug release

Introduction

Cancer is uncontrolled cell growth that can spread to other body regions. Death may result if the spread of the cells is not stopped. Chemotherapy, radiation therapy, surgery, hormonal, immunologic, and targeted therapies (drugs that specifically target the growth of cancer cells) are some of the already recommended treatments [1].

✉ Moshera Samy
moshera_samy1984@yahoo.com

1 Polymers and Pigments Department, National Research Centre, Dokki, Giza 12622, Egypt

Most anticancer medications attack all rapidly developing cells, including healthy cells, without distinguishing between cancer and normal cells; as a result, they can seriously affect the patient's health [2]. The effectiveness of treatment is additionally constrained by the medications' high toxicity, limited therapeutic window, and low solubility [3].

5-Fluorouracil (5-FU) is a pyrimidine analogue that belongs to the broad-spectrum anticancer drugs and acts as an antimetabolite. When used alone or in combination with other anticancer medications, it exhibits broad-spectrum effectiveness against the brain, head, ovary, neck, breast, pancreas, liver, gastrointestinal tract tumors [4–6]. 5-FU can be incorporated into RNA and DNA because of its structure. It acts as a thymidylate synthase inhibitor [7]. The 5-FU has drawbacks, including nonspecificity that can cause systemic toxicity, wide dispersion, extremely low absorption, short half-life, and the need for high doses that can result in adverse effects [8]. Additionally, the clinical usage of 5-FU has been severely constrained by the development of resistance by tumor cells [8, 9]. Additionally, the clinical usage of 5-FU has been severely constrained by the development of resistance by tumor cells [8, 9]. The 5-FU is incorporated into polymeric nanofibers in order to get over the above-mentioned drawbacks, These drug carriers are special in that they allow for simple surface property adjustment, can shield the drug when it is encapsulated, and can enhance the drug stability [10]. The fibers can be treated with 5-FU using techniques like coating and dipping. Other methods exist for loading the drug into the nanofibers [11]. It should be mentioned that among the various carriers, nanostructures have recently demonstrated their ability for targeted drug delivery [12]. Due to their high flexibility, porosity, and superficial, mechanical properties [13, 14], nanotechnology and electrospun nanofiber mats have created new opportunities for drug delivery [15] for the majority of diseases.

Nanofibers with high porosity and a particular surface area, which resemble the extracellular matrix, can be made using the straightforward electrospinning method [16, 17]. A jet of polymer solution is subjected to a high voltage to create electrospun nanofibers. Polymeric nanofibers, as a result, are accumulated on the target collector [18]. The best nanofiber morphology may be created by modifying variables including tip-to-collector distance, voltage, solute concentration variation, and solvent type [17, 19]. A jet of polymer solution is subjected to a high voltage to create electrospun nanofibers. Polymeric nanofibers, as a result, are accumulated on the target collector [18]. The best nanofiber morphology may be created by modifying variables including tip-to-collector distance, voltage, solute concentration variation, and solvent type [17, 19].

Several opportunities exist to enhance drug efficacy and pharmacological performance parameters using new drug delivery systems based on biodegradable polymers. An ideal and targeted drug delivery system to the cancer cell infested site needs to be developed. This is considering that reduced toxicity, enhanced chemical and physical qualities, defense against chemical degradation, and increased environmental sustainability are some of these factors [20, 21].

Poly(ε-caprolactone) (PCL) biodegradable synthetic polymers have gained attention in the biomedical field, including as drug carriers, over the last two decades [22–24], because it has excellent biodegradability, biocompatibility,

biodegradability, fiber-forming capability, and good mechanical properties [25]. However, the hydrophobicity, lack of natural cell-specific recognition sites [26], and slow degradation kinetics of PCL [27] may limit it from being used in a variety of biomedical applications that require a faster rate of absorption [28]. To get over this limitation, PCL is mixed with other natural sources of hydrophilic polymers or proteins like gelatin, lecithin, and chitosan, all of which can improve the hydrophilicity and biocompatibility of the resulting PCL nanofiber mats [29, 30]. Gelatin contains the amino acids glycine, proline, and hydroxyproline, which collectively help cells adhere to one another. The Gel is non-antigenic and has good porosity, biocompatibility, fluid retention characteristics, and cell-specific binding sites [31]. Gel has limited mechanical strength and degradability [32]. An immunogenic response is triggered when human skin fibroblasts are exposed to electrospun nanofibers of synthetic polymers, but this can be reduced by coaxially electrospinning with gelatin [33]. So, by mixing PCL with gelatin, it is possible to produce scaffolds that are both mechanically stable and feature cell-specific patterns that are appropriate for both tissue engineering and rapid wound healing. Polycaprolactone nanofibers mats are widely used in biomedical applications. The least toxic solvent system among several others was found to be the formic acid/acetic acid (FA/AA) system. The FA/AA solvent system was referred to as be the safest solvent system for electrospinning PCL/Gel nanofibers since it was found to produce uniform, beadless, reproducible PCL/Gel nanofibers with a small nanofiber diameter compared to other solvents. In addition, it is commonly utilized as a solvent for several polymers, including gelatin and chitosan. In the present work, the effect of encapsulating different concentrations of 5-FU into PCL/Gel NFs mats was investigated using SEM, FTIR, TGA, and XRD to improve the stability of the polymer solution as well as the resulting properties of the electrospinning mats such as hydrophilicity.

Experimental

Materials

Poly(ε-caprolactone) (99.9%, average molecular weight 80,000 gm/mol, Sigma-Aldrich, Germany), formic acid (85%, Edwic, Egypt), acetic acid (96%, Edwic, Egypt) and 5-fluorouracil (5-FU; $C_4H_3FN_2O_2$; 5-fluoropyrimidine-2,4-dione, 99%, Alfa Aesar, Germany), and disodium hydrogen orthophosphate (Na_2HPO_4) were obtained from Sigma-Aldrich, Germany. Potassium hydrogen phosphate (KH_2PO_4) was purchased from Alpha Chimika, India, Gelatin (BDH, catalog number: 440454B, Biomolecules, India). All other chemicals, unless otherwise specified, are of analytical grade. They were used as purchased without any purification.

Electrospinning of PCL/Gelatin nanofibers

For the formation of the PCL solution, 20 wt.% PCL were dissolved in a solvent mixture of 70:30 FA/AA and stirred magnetically for up to three hours to achieve

complete dissolution. For solution for 5-FU-PCL/Gel NFs mats, 20 wt.% PCL was prepared as mentioned above. Then, 0.02 gm of gelatin was added, and the amount of 5-fluorouracil (5-FU) was added and magnetically stirred until dissolution. Three different concentrations of 5-FU (5, 10 and 15 wt.%) were used and termed as follows: (5%) 5-FU-PCL/Gel NFs, (10%) 5-FU-PCL/Gel NFs, and (15%) 5-FU-PCL/ Gel NFs, respectively. After that, a 21G needle was used to inject the prepared PCL and 5-FU-PCL/Gel NFs solutions into a 1 ml syringe at a tip-to-collector distance of 12 cm while operating under a 20 kV applied voltage. The Glassman High Voltage Series encompassing the range of 0–20 kV was used to adjust the voltage. The Syringe Pump Series 100 controls the solution's flow rate. At a relative humidity (RH) of $60 \pm 2\%$ and a room temperature of about 22 °C, electrospinning was done. The appropriate diameter was then achieved by rolling up the manufactured PCL-Gel NFs mats.

Analysis of 5-FU

Determination of the maximum wavelength of absorption (λ_{max}) of 5-FU

Using 5-FU in phosphate buffer solution (PBS) as a solvent, the spectrophotometric assay for 5-FU analysis was carried out using a Shimadzu UV spectrophotometer (2401/PC, Japan). With PBS serving as a blank, the 5-FU dissolved in the studied solvent at 10 g/ml was screened to detect the λ_{max} of 5-FU from the UV spectrum. This concentration was made by diluting a stock solution of 10 µg/ml, which was made by properly weighing 10 mg of 5-FU and dissolving it in 10 ml of the PBS.

Formation of 5-FU calibration curve

Using the proper dilutions of the above-mentioned stock solution, six concentrations of 5-FU 4, 6, 8, 10, 12, 14, and 16 µg/ml were prepared in PBS solvent. Each of these concentrations' absorbance was measured at the λ_{max} using PBS as a blank. The concentration of 5-FU and the UV absorbance at the appropriate wavelength of maximum 5-FU absorption in the PBS as a solvent were plotted on a linear calibration curve.

Determination of encapsulation efficiency (EE%)

In order to determine the EE% of 5-FU in the prepared nanoparticles, the combined washings after centrifugation were appropriately diluted using 0.5% acetic acid. The amount of free, unencapsulated 5-FU was measured spectrophotometrically at 265.2 nm using the regression equation of the standard calibration curve plotted employing suitable concentrations of 5-FU [34]. The amount of encapsulated 5-FU was determined by difference between the amount of free, unencapsulated 5-FU in the combined washings and the initial amount used in preparation of PCL/Gel NFs where the following equation was employed [35, 36]:

$$EE\% = \frac{Free\ drug - Total\ drug}{Total\ drug} \times 100 \tag{1}$$

Characterization of 5-FU loaded PCL/Gel NFs mats

Fiber morphology

Fiber morphology was investigated under a field emission scanning electron microscope SEM using Quanta FEG 250 (FEI Company, Holland) device. The diameter distribution of the electrospun nanofibers was calculated by measuring about 80–100 individual fibers with image analysis software (Image J 1.42q software (NIH, Bethesda, Maryland, USA).

Fourier transform infrared spectroscopy (FTIR)

FTIR spectroscopy was used to study the composition of gelatin, PCL, and 5-FU as well as the changes in the functional groups of electrospun PCL/Gel NFs mats due to the encapsulation of 5-FU. An FTIR spectrometer (Jasco, FT/IR 6100, Japan) was used to record the spectra. The powdered samples were ground and combined with KBr and then, compacted into disks using the KBr pellet process. A 4000–400 cm^{-1} scanning range was used.

X-ray diffraction (XRD)

The crystalline structure and amorphousness of Gel, 5-FU, pure PCL, the electrospun PCL/Gel NFs mats and 5-FU loaded PCL/Gel NFs mats were evaluated using X-ray diffraction. Measurements were acquired with an X-ray diffractometer (Bruker AXS, D8 Advance, Germany), which was operated at 40 kV and 40 mA using CuKα as a radiation source where $\lambda = 1.54$ Å. The diffractograms were recorded in the diffraction angle (2θ) range between 5 and 65°, with a scanning rate of 5°/min.

Thermal gravimetric analysis (TGA)

The thermal behavior of 5-FU-PCL/Gel NFs samples was measured using the thermal analyzer TGA-SDT Q600 V20.9 Build 20, (USA) in the temperature range of room temperature to 900 °C at a heating rate of 10 °C/min in an inert nitrogen atmosphere (N$_2$) using reference alumina.

Differential scanning calorimetry (DSC)

Thermal stability of 5-FU-PCL/Gel NFs was investigated through DSC using thermal analyzer DSC–SDT (Simultaneous DSC-TGA) Q600 V20.9 Build 20, (USA) in the range from room temperature to 350 °C at a heating rate of 10 °C/min under inert

nitrogen atmosphere (N_2) using reference alumina. The samples weight was between 2.5 and 12 mg.

In vitro drug release study

In order to allow the electrospun nanofiber mats (5-FU-PCL/Gel NFs) to release drug in phosphate buffer solution (PBS), it was cut into roughly similar sizes (10×10 mm) immersed into 14 ml of 0.01 M PBS, pH 7.4 in a closed centrifuge tubes and then, kept in a shaking incubator at 37 °C to allow the NFs to release drug in PBS. At predetermined time intervals (0, 20, 40, 60, 80, and 100 h), 5 ml of the release medium was withdrawn and replaced with 5 ml of fresh buffer solution. Then, calculate the amount of drug released from nanofibers during that time. The samples were properly diluted before being spectrophotometrically examined for 5-FU concentration. Nine solutions of 5-FU at various known concentrations were used to calibrate the 5-FU concentration. The proportion of released 5-FU to 5-FU that was first injected into the dialysis bag was used to calculate the cumulative percentage of drug released. A triple of each measurement was done.

Drug release kinetics

Kinetic analysis of drug release of 5-FU from different PCL/Gel NFs was performed using different mathematical models, including zero-order and first-order models, Higuchi's model, Hixson-Crowell cube root law, Baker-Lonsdale equation of time kinetics, and the Peppas exponential model, the correlation coefficients values (R^2) were calculated from the plots of Q versus t in case of zero order, $\log(Q_0 - Q)$ versus t for first order, Q versus $t^{1/2}$ for Higuchi model, $Q_0^{1/3} - (Q_0 - Q)^{1/3}$ versus t for Hixson-Crowell model, $3/2[1 - (1 - Q/Q_0)^{2/3}]$ versus t for Baker-Lonsdale model, and Q versus Log t for Peppas model. Where (Q) indicates the amount of drug released at time (t), and ($Q_0 - Q$) indicates the amount of drug still present at that time (t). To ascertain the drug release mechanism, the release exponent (n) in the Peppas model was also determined.

Statistical analysis

The experimental results were presented as mean value $\pm$ standard deviations (SD). Statistical analysis was performed by means of a two-way analysis of variance (ANOVA). All experiments were repeated at least three times. The statistical significance of the differences was evaluated by two-way analysis of variance, and $P < 0.05$ was considered to indicate a statistically significant difference.

Results and discussion

Fiber morphology characterization

The Fig. 1 demonstrates SEM images of electrospun pure PCL NF mats, PCL/Gel NF mats, and the fabricated 5-FU-PCL/Gel NF mats prepared from PCL mixed with Gel at different concentrations of 5-FU (5, 10, and 15 wt.%) and their fiber distribution. All fibers are nanoscale and exhibit uniform and smooth morphology [37, 38]. Figure 1a shows that the pure PCL NFs mat fibers are uniformly and randomly oriented with no beads or bundles of fibers, with an average nanofibers diameter of 223.2 ± 57.6 nm. The average diameters of nanofibers were about 72.8 ± 10.2 nm (Fig. 1b). The difference in diameter between PCL and the other samples could be attributed to the inclusion of Gel, which reduced the spinning solution's viscosity [38, 39]. SEM Images of the NFs mats are shown in Fig. 1c–e. The average nanofiber diameters of (5%) 5-FU-PCL/Gel NFs, (10%) 5-FU-PCL/Gel NFs & (15%) 5-FU-PCL/Gel NFs mats were found to be in the range of 96.6 ± 25.9, 97.2 ± 16.5, and 100 ± 32.8 nm, respectively. 5-FU was encapsulated into the core of the NFs during the electrospinning process using the FA/AA solvent system. Increasing the 5-FU content, bead-free fibers and an increase in nanofiber diameter were produced, as shown in Table 1. The NF mats were randomly distributed and showed non-uniform surface features with many 5-FU particles attached to the surface. The SEM image did not show large beads as in PCL NFs, but it showed some fiber bundles within the nanofiber matrix, which indicated some 5-FU particles attached to the surface of NFs mats. Due to the higher viscosity, the polymeric chains are more conjugated with each other and form thicker fibers. The diameter of the resulting nanofiber mats can vary depending on the 5-FU concentration of the electrospun target. The findings confirm those of Iqbal et al. [40].

Encapsulation efficiency (EE%)

In this study, the EE% of (5%) 5-FU-PCL/Gel NF, (10%) 5-FU-PCL/Gel NF and (15%) 5-FU-PCL/Gel NF mats were found to be in the range of 53.3%, 61.8%, and 67.6%, respectively. It is clear that an increase in EE% (P b0.05) was observed with the increase in 5-FU concentration from 5 to 15 wt. investigated. This finding comes in agreement with previous reports. For example, Nagarwal et al. reported an increase in EE% upon increasing 5-FU concentration from 5 to15 wt.% The values obtained suggest the high efficiency of the encapsulation and the suitability of the nanoplatform for use in drug delivery applications. This sample was selected for controlled release testing [41].

FTIR analysis

The chemical composition of the nanofiber mats and the presence of each component in the miscible fiber mixtures were investigated using FTIR analysis.
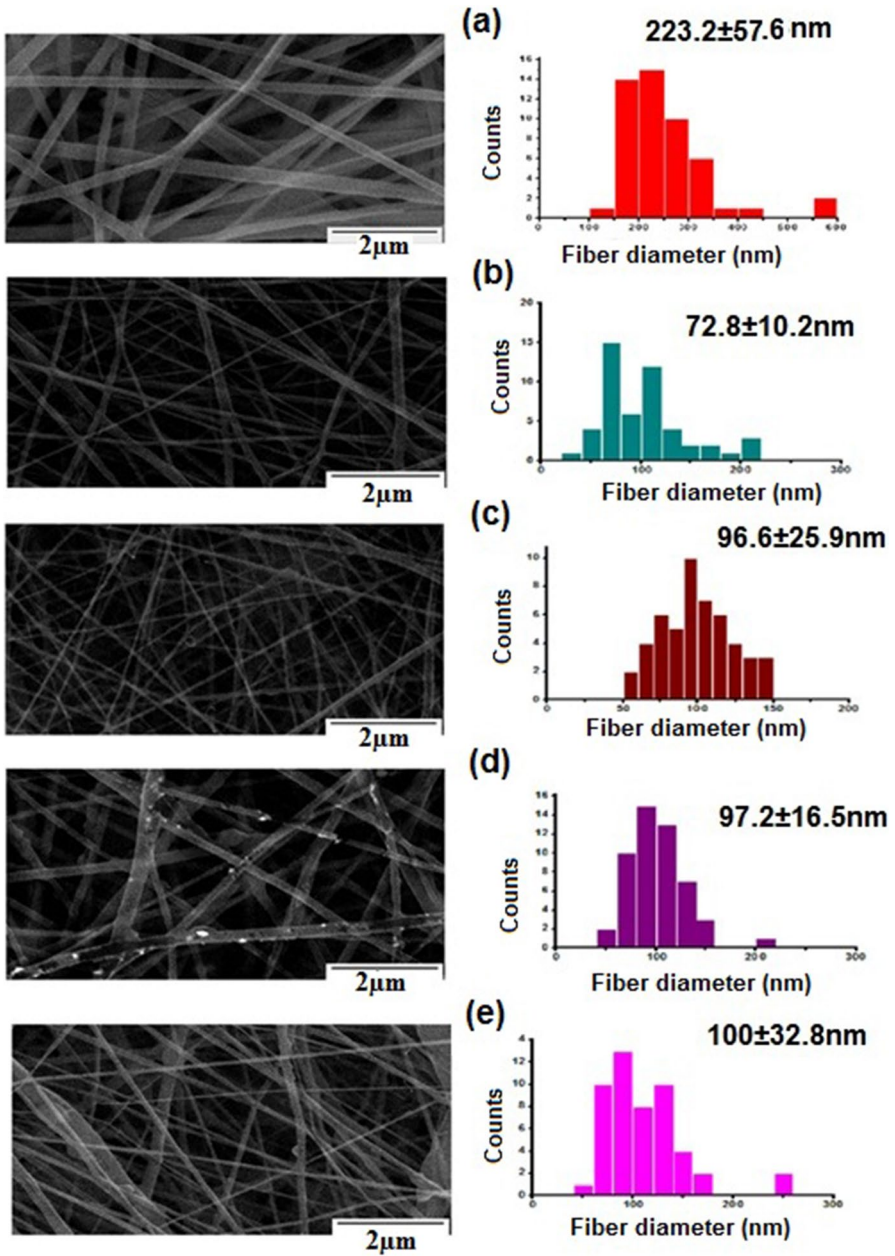
Fig. 1 SEM images of electrospun for (**a**) pure PCL NF, (**b**) PCL/Gel NF mats, (**c–e**) 5-FU-PCl/Gel NF mats at various 5-FU concentrations (5%, 10%, and 15%), and nanofiber diameter distribution histograms, respectively (scale bar = 2 μm)

Table 1 5-FU concentration and electrospun NanoFiber Diameter

Sample name	PCL concentration	5-FU concentration	Electrospun nanofiber diameter (nm)
PCL NFs	20%	–	223.2 ± 57.6
PCL/Gel NFs		–	72.8 ± 10.2
(5%) 5-FU-PCL/Gel NFs		5%	96.6 ± 25.9
(10%) 5-FU-PCL/Gel NFs		10%	97.2 ± 16.5
(15%) 5-FU-PCL/Gel NFs		15%	100 ± 32.8

Figure 2 shows the FTIR spectra of Gel, PCL, 5-FU, PCL/Gel nanofiber mats, and 5- FU-PCL/Gel NFs mats ((5%) 5-FU-PCL/Gel NFs, (10%) 5-FU-PCL/Gel NFs and (15%) 5- FU-PCL/Gel NFs). The FTIR spectra of gelatin show a band at 3262.15 cm^{-1} which corresponds to the N–H stretching vibration: 1627.93 cm^{-1}, which corresponds to C=O stretching vibration of preprimary amide; 1524.71 and 1444.98 cm^{-1} represent the bending vibration of secondary amide (N–H and –CH$_2$); 1238.49 and 1028.34 cm^{-1} due to the N–H bending vibration and the C=O stretching vibration of tertiary amide [42, 43]. FTIR spectral analysis of PCL revealed an intense peak at 1724.64 cm^{-1} and a small band at 731.12 cm^{-1} corresponding to the ¯C=O stretching of the ester carbonyl group of PCL. The peaks at 2866.79 and 2941.17 cm^{-1} correspond to the C-H bond of the saturated carbons [43, 44]. Due to the vibration of the aromatic ring and imide stretch (secondary amide and tertiary amide), 5-FU exhibits characteristic bands at 3178.2, 1725.1, 1655.4, 1426.1, 1245.6, 809.8, and 546.8 cm^{-1}. –C–H stretching bands cause the spectral bands at $3025.7 - 2928.3$ cm^{-1}, and pyrimidine vibration causes the peak at 1348.1 cm^{-1}. In addition, at 1179.2, 1655.5, and 1245 cm^{-1}, respectively, the –C–O and –C–N vibrations were seen [45]. The characteristic bands of PCL at 2867.27 and 2944.59 cm^{-1} correspond to –CH$_2$ symmetric and asymmetric –CH$_2$ vibrations; 1724.50 cm^{-1} represents the C=O stretching of the ester group; 1047.26 and 1239.16 cm^{-1} refer to symmetric and asymmetric –C–O–C stretching vibrations, respectively. In the spectral of 5-FU- PCL/Gel NFs mats, at 1725.3 and 1672.4 cm^{-1}, the carbonyl stretching (C=O) bands of PCL and 5-FU, respectively, were observed. At 2944.59 cm^{-1}, the 5-FU-PCL/Gel NFs' C–H group stretching band could be seen. In the spectra of 5-FU, the C-F stretching band had a peak of 1293.6 cm^{-1} [20, 46]. The fact that this band was seen at 1293.6 cm^{-1} shows that the drug was loaded effectively. The electrospun 5-FU-PCL/Gel NF mats also showed the distinctive PCL, gelatin, and 5-FU bands. Additionally, the electrospun 5-FU- PCL/Gel NF mats showed the distinctive bands of PCL, gelatin, and 5-FU, indicating that the individual components had been successfully incorporated into the resulting nanofiber mats.

XRD

XRD patterns were recorded between 5° and 65° for Gel, PCL, 5-FU, electrospun PCL/Gel NF mats, and 5-FU-PCL/Gel NF mats at various 5-FU concentrations.
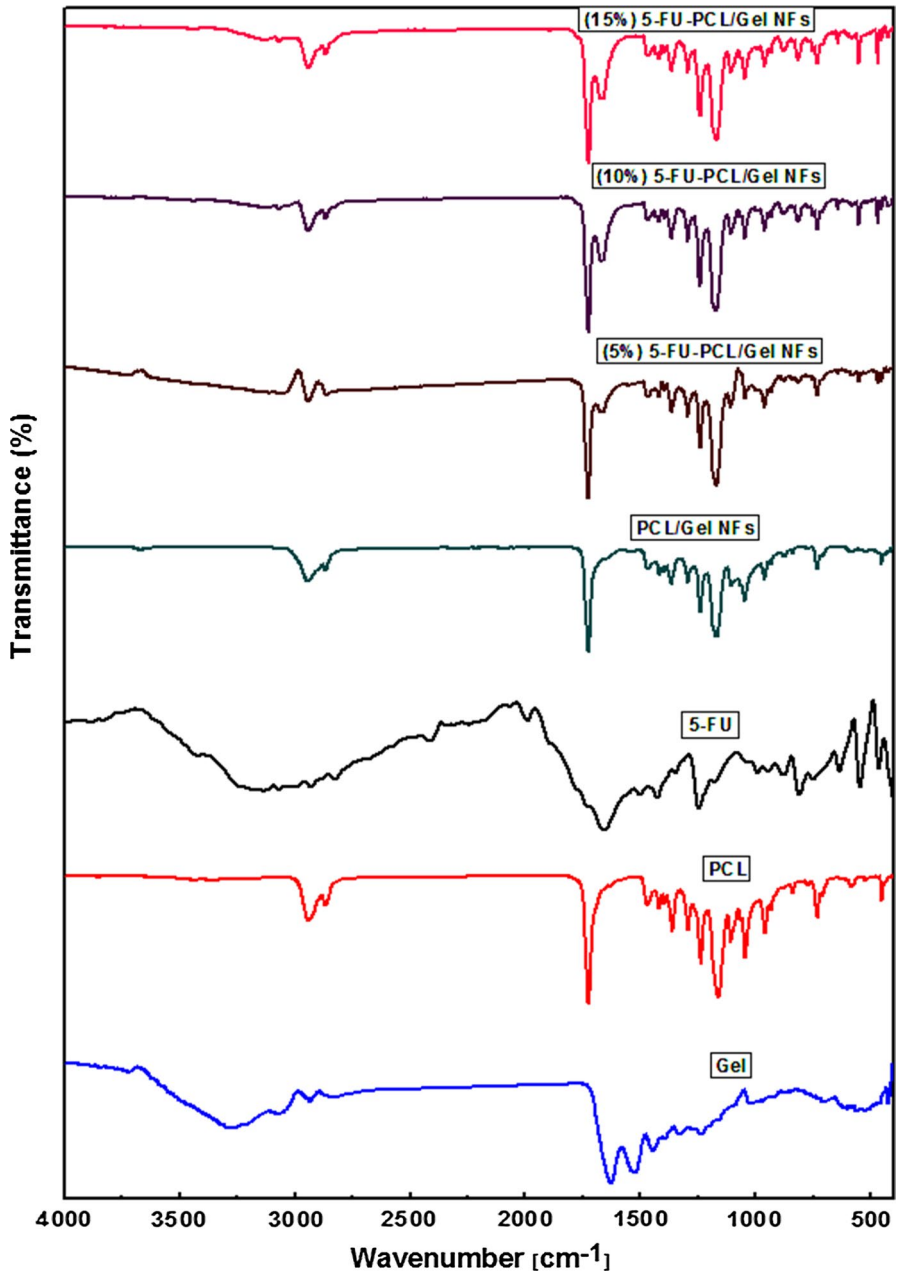
Fig. 2 FTIR spectra of Gel, PCL, 5-FU, PCL/Gel NF mats, and 5-FU-PCL/Gel NF mats for different concentrations of 5-FU are (5%) 5-FU-PCL/Gel NF, (10%) 5-FU-PCL/Gel NF, and (15%) 5-FU-PCL/Gel NF, respectively
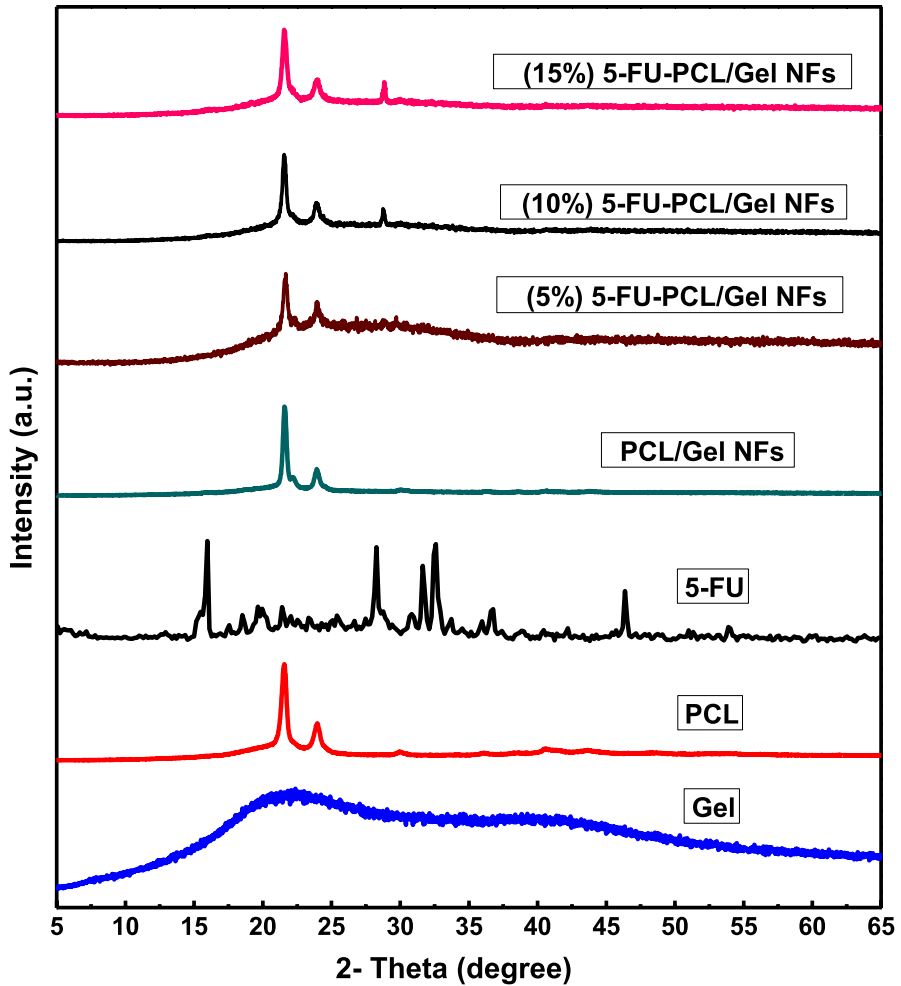
Fig. 3 XRD patterns of Gel, PCL, PCL/Gel NF mats, and 5-FU-PCL/Gel NF mats at different 5-FU concentrations are (5%) 5-FU-PCL/Gel NF, (10%) 5-FU-PCL/Gel NF and (15%) 5-FU-PCL/Gel NF, respectively

XRD used to investigate their crystalline structures [47] and determine how 5-FU affects it (Fig. 3). Gel has no significant peak in its XRD pattern, indicating the amorphous nature of Gel [48]. Two distinct diffraction peaks in the PCL were seen at Bragg angles of $2\theta = 21.5°$ and $23.9°$, indicating that of the PCL. Pure 5-FU's diffraction pattern revealed strong at $2\theta = 16.2, 19.8, 21.6, 22.1, 28.3, 32.7, 36.7, 36.8,$ and $46.5°$, indicating that a drug is in a crystalline state [49]. PCL/Gel NF mats and 5-FU-PCL/Gel NF mats diffracted at $2\theta = 21.6°$ and $23.8°$, respectively [50, 51]. However, after loading 5-FU into PCL/Gel NFs, all characteristic peaks disappeared completely. The result indicates that the crystallinity of 5-FU is significantly reduced in PCL/Gel NF mats thereby existing in an amorphous form. The position of the

PCL diffraction peaks in the XRD pattern was shifted to the right and had much less intensity than those of the pure PCL nanofibers, showing a different crystal form and a lower degree of crystallinity of the electrospun PCL/Gel nanofibers.

TGA

The Fig. 4 shows thermograms of Gel, PCL, 5-FU, PCL/Gel NFs, and 5-FU-PCL/Gel NFs as (5%) 5-FU-PCL/Gel NFs, (10%) 5-FU-PCL/Gel NFs, and (15%) 5-FU-PCL/Gel NFs, respectively. Gel has three stages of thermal degradation. The first step (50–200 °C) is because of the loss of moisture (absorbed and bound). The second step (200–390 °C) is because of the main zone of thermal degradation which occurs between peptide bond breakage and protein chain breakage, and the third step is about 400 °C, which is due to thermal decomposition [52, 53]. PCL displays one thermal degradation step (390–450 °C) with a weight loss of 88%. The results are in agree with previous findings on the thermal degradation of PCL [54]. 5-FU exhibits two thermal degradation steps. The degradation step takes place between 280 and 340 °C, losing 10 and 86% of its weight, respectively, which can be attributed to the loss of water [53]. PCL/Gel NF mats and all samples of 5- FU-PCL/Gel NFs ((5%) 5-FU-PCL/Gel NFs, (10%) 5-FU-PCL/Gel NFs, and (15%) 5-FU-PCL/Gel NFs) decomposed in a thermal
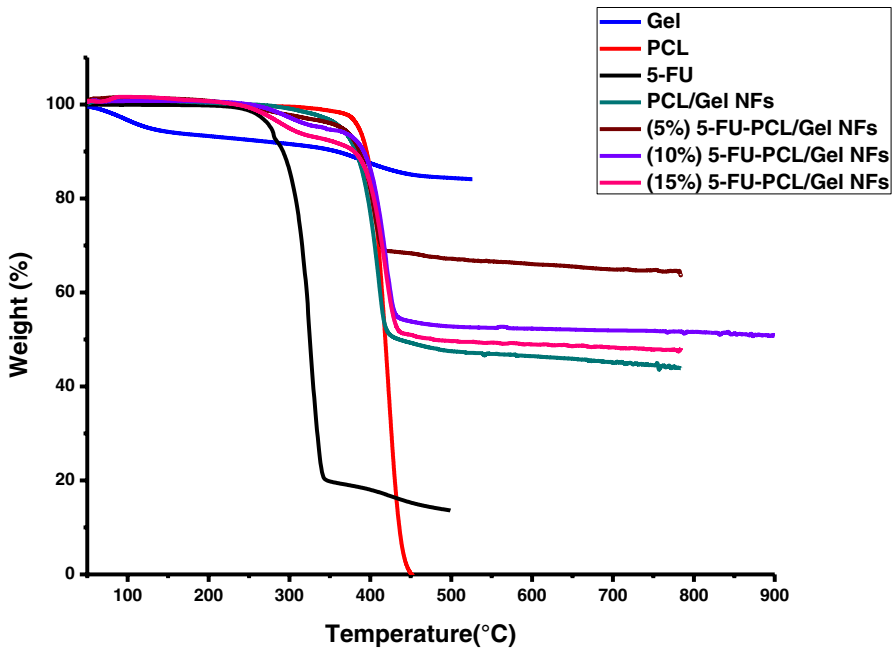

Fig. 4 TGA thermograms of Gel, PCL, PCL/Gel NF mats, and 5-FU-PCL/Gel NF mats for different concentrations of 5-FU are (5%) 5-FU-PCL/Gel NFs, (10%) 5-FU-PCL/Gel NFs and (15%) 5-FU-PCL/Gel NFs, respectively

degradation phase (350–450 °C) losing 96.4% of its weight. This proves that by combining with PCL, gelatin was thermally stabilized. Additionally, compared to pure PCL, both PCL/Gel NF and 5-FU-PCL/Gel NF mats show decreased thermal stability. This is because the nanofibers have a bigger surface area and higher reactivity than the polymer, which increases the thermal degradation to occur more quickly. The literature [44] reported a similar observation, which supported the findings of the XRD investigation.

DSC

DSC is essentially used to measure enthalpy variations according to the changes in the thermal properties of the material as a function of time or temperature. The final melting temperatures and enthalpy changes were elucidated from DSC thermograms as indicated in Fig. 5. The DSC curve of PCL/Gel showed Tm = 61.6 °C, while the DSC curve of 5-FU exhibits endothermic peak at the temperature of 282.80 °C corresponding to its melting point [26]. The thermogram of the drug-loaded nanofiber has an endothermic peak at about 61.6 °C associated with the melting of the PCL/GeL [55], and a broad endothermic peak in the range of 125–200 °C that is related to loss of absorbed moisture by the 5-FU. Another endothermic peak at about 282,8 °C is for the drug melting. The DSC graph of 5-FU–PCL/Gel NFs confirms the appropriate distribution of the 5-FU drug in PCL/GeL nanofibers which agree with the literature [56].

5-FU analysis method

The determination of the λ_{max} of 5-FU began with screening 5-FU using phosphate buffer at PH 7.4 over an UV spectroscopic scan (200–400 nm). As seen in Fig. 6, by diluting the stock solution of 10 µg/ml and different concentrations of 5-FU in 4, 6, 8, 10, 12, and 14 µg/ml in PBS, standard solutions in the range of 4–14 µg/ml were produced, and the absorbance of each of these concentrations was measured at the appropriate λ_{max} for the PBS.

Formation of calibration curve of 5-FU

A calibration curve was drawn in Fig. 7, in the concentration range of 4–14 µg/ml by plotting absorbance and concentration on the Y and X axes, respectively. Using phosphate buffer as a blank [49], the λ_{max} of 5-FU was found to be 266.2 nm, which demonstrates the accuracy and dependability of the assay for determining the concentration of 5-FU. Regression equations ($y = 0.0452x + 0.0014$) and linear regression with correlation coefficient $R^2 = 0.9983$ show that a linear relationship between the concentration of 5-FU and UV absorbance was established. It was determined that the slope was 0.0452.
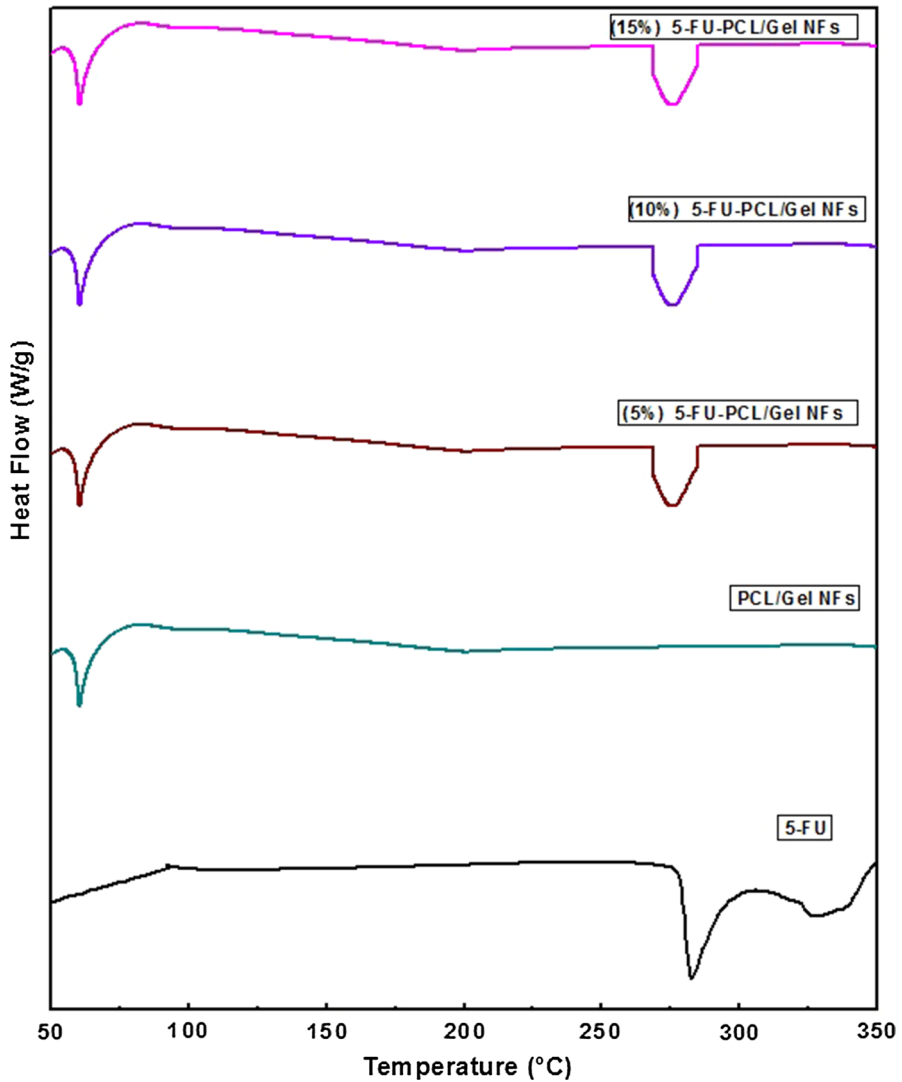
Fig. 5 DSC thermograms of 5-FU, PCL/Gel NF mats, and 5-FU-PCL/Gel NF mats for different concentrations of 5-FU are (5%) 5-FU-PCL/Gel NFs, (10%) 5-FU-PCL/Gel NFs and (15%) 5-FU-PCL/Gel NFs, respectively

Drug release behavior

The percentage of released 5-FU from PCL/Gel NF mats was examined. By using a spectrophotometer, the maximum absorbance wavelength wave of 5-FU in phosphate buffer was found to be 266.2 nm [57]. Figure 8 displays in vitro 5-FU release profile from three prepared PCL/Gel NF mats: (5%) 5-FU-PCL/Gel NF, (10%) 5-FU-PCL/Gel NF, and (15%) 5-FU-PCL/Gel NF mats, respectively. The examined
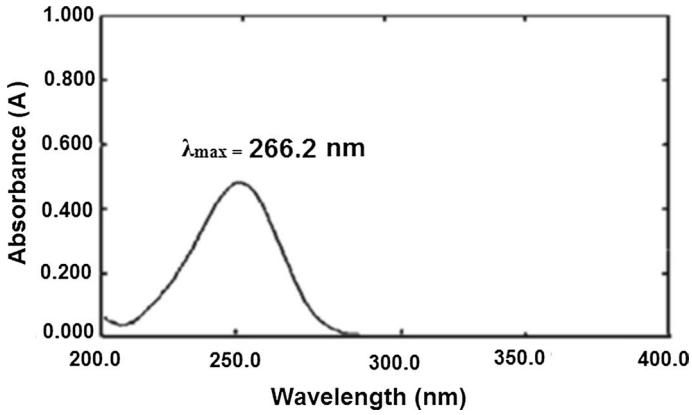
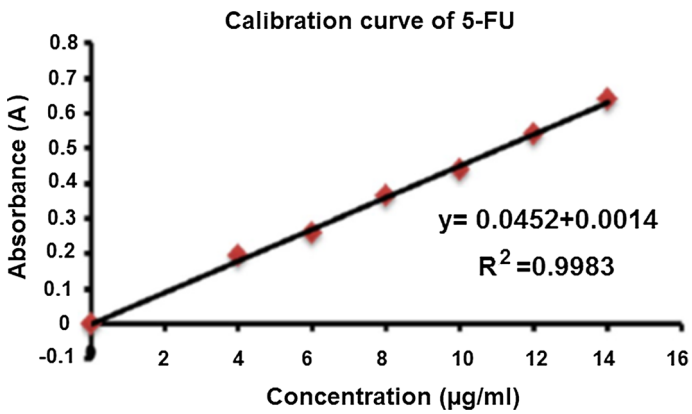**Fig. 6** UV absorbance spectra of 5-FU in PBS (PH 7.4) by using UV spectrophotometer

Fig. 7 Calibration curve of 5-FU in phosphate buffer (PH 7.4) prepared by using UV spectrophotometer
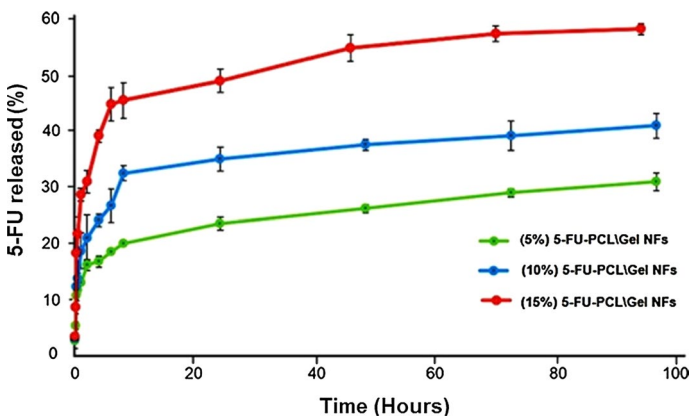

Fig. 8 In vitro 5-FU release profile from the 5-FU loaded PCL/Gel NFs mats in PBS (PH 7.4) at 37 °C

Table 2 5-FU release kinetics from the electrospun PCL/Gel NF mats

Sample name	n	SD	Release kinetics
(5%) 5-FU-PCL/Gel NFs	0.042	0.015	Fickian
(10%) 5-FU-PCL/Gel NFs	0.063	0.017	Fickian
(15%) 5-FU-PCL/Gel NFs	0.081	0.033	Fickian

Table 3 R^2 of the electrospun PCL/Gel NF mats is derived from the 5-FU release profile

Sample name	Zero order R^2	First order	Higuchi
(5%) 5-FU-PCL/Gel NFs	0.821 ± 0.064	0.970 ± 0.026	0.924 ± 0.021
(10%) 5-FU-PCL/Gel NFs	0.716 ± 0.032	0.947 ± 0.003	0.924 ± 0.023
(15%) 5-FU-PCL/Gel NFs	0.835 ± 0.025	0.964 ± 0.0018	0.949 ± 0.016

PCL/Gel NFs mats release profiles displayed a biphasic tendency, with an initial fast release being seen for the first hours. A persistent, gradual release that persisted for up to 100 h followed this. This 5-FU slow-release behavior has been described in PCL/Gel NFs before [46]. Another interesting finding is that, after 100 h, when the concentration of 5-FU declined, the percentage of medicine that was released considerably increased. An increase in the 5-FU concentration was linked to a more prolonged release profile in the case of PCL-based nanofibers, where a similar behavior related to the 5-FU concentration was identified [58, 59]. The results confirmed that the nanofibers mats have a sustained 5-FU release.

Drug release kinetics

The Fickian release mechanism was followed by the diffusion index for all PCL/ Gel NF mats with 5-FU loaded in Table 2. As a result, the drug release from the mats was crucial to the delivery of the drug. Three electrospun 5-FU-PCL/Gel NFs at various 5-FU concentrations were used to calculate the correlation coefficients of the Zero-order, First-order, and Higuchi models in order to identify the mechanism model of the release of 5-FU from the constructed electrospun 5-FU-PCL/Gel NFs mats. Table 3 presents the findings. It has been described that the Higuchi model will be accurate when the release rate of the 5-FU from the PCL/Gel NFs is significantly higher than the degradation rate of PCL and let it be done mostly via diffusion from the pores of the polymer [60]. The drug release from this sample follows the Higuchi model since 5-FU has a very high hydrophilicity and PCL degrades slowly. Statistical findings, for (5%) 5-FU-PCL/Gel NF, (10%) 5-FU-PCL/Gel NF, and (15%) 5-FU-PCL/Gel NF mats, respectively, the average correlation coefficient of the First-order and Higuchi models does not differ significantly. As a result, we can conclude that the 5-FU-PCL/Gel NFs' drug release mechanism also adheres to Higuchi's First-order model. When drugs are released under conditions of polymer breakdown and dispersion, the first-order model applies [53].

Conclusions

5-FU-PCL/Gel NF mats were manufactured successfully with changes in the percentage of 5-FU at (5, 10, and 15 wt.%) by using electrospinning with 20% PCL. The effect of loading 5-FU into the PCL/Gel NFs was investigated in the present study. The hydrophilicity of the resulting electrospun PCL-Gel NFs mats is improved by loading 5-FU into the PCL nanofibers solution, which also greatly increases its stability in its polymeric system. The chemical interaction between PCL, gelatin, and 5-FU in the electrospun PCL-Gel NF mats was examined using FTIR, TGA, and XRD. The observed SEM data showed that the fiber diameter increased with increasing 5-FU concentration, Also, it was deduced that the addition of 5-FU into PCL/Gel NFs will be a further candidate for biomedical applications. In addition to the Higuchi model, the drug release mechanism in each sample followed a Fickian release and the First-order model. According to the study's findings, the PCL/Gel NFs with 5-FU as a model drug have the potential for regulated drug release.

Data availability The raw data required to reproduce these findings are available from the corresponding authors upon request.

Declarations

Conflicts of interest The authors report no conflicts of interest.

References

1. Siegel RL, Miller KD, Jemal AJC (2015) Cancer statistics. 65:5–29
2. Bromberg L, Alakhov V (2003) Effects of polyether-modified poly (acrylic acid) microgels on doxorubicin transport in human intestinal epithelial Caco-2 cell layers. J Controll Release 88(1):11–22
3. Pulkkinen M, Pikkarainen J, Wirth T, Tarvainen T, Haapa-aho V, Korhonen H, Järvinen K (2008) Three-step tumor targeting of paclitaxel using biotinylated PLA-PEG nanoparticles and avidin–biotin technology: formulation development and in vitro anticancer activity. Eur J Pharm Biopharm 70(1):66–74

4.	Nivethaa EAK, Dhanavel S, Rebekah A, Narayanan V, Stephen A (2016) A comparative study of 5-Fluorouracil release from chitosan/silver and chitosan/silver/MWCNT nanocomposites and their cytotoxicity towards MCF-7. Mater Sci Eng C 66:244–250

5.	Salerno A, Domingo C, Saurina J (2017) PCL foamed scaffolds loaded with 5-fluorouracil anti-cancer drug prepared by an eco-friendly route. Mater Sci Eng C 75:1191–1197

6.	Tummala S, Kumar MS, Prakash A (2015) Formulation and characterization of 5-Fluorouracil enteric coated nanoparticles for sustained and localized release in treating colorectal cancer. Saudi Pharm J 23(3):308–314

7.	Arias JL (2008) Novel strategies to improve the anticancer action of 5-fluorouracil by using drug delivery systems. Molecules 13(10):2340

8.	Zhang N, Yin Y, Xu SJ, Chen WS (2008) 5-Fluorouracil: mechanisms of resistance and reversal strategies. Molecules 13(8):1551–1569

9.	Arias JL, Ruiz MA, López-Viota M, Delgado ÁV (2008) Poly (alkylcyanoacrylate) colloidal particles as vehicles for antitumour drug delivery: a comparative study. Colloids Surf B Biointerfaces 62(1):64–70

10.	Sahle FF, Balzus B, Gerecke C, Kleuser B, Bodmeier R (2016) Formulation and in vitro evaluation of polymeric enteric nanoparticles as dermal carriers with pH-dependent targeting potential. Eur J Pharm Sci 92:98–109

11.	Szentivanyi A, Chakradeo T, Zernetsch H, Glasmacher B (2011) Electrospun cellular micro-environments: Understanding controlled release and scaffold structure. Adv Drug Deliv Rev 63(4–5):209–220

12.	Zhang L, Gu FX, Chan JM, Wang AZ, Langer RS, Farokhzad OC (2008) Nanoparticles in medicine: therapeutic applications and developments. Clin Pharmacol Therap 83(5):761–769

13.	Cacciotti I, Chronopoulou L, Palocci C, Amalfitano A, Cantiani M, Cordaro M, Arcovito A (2018) Controlled release of 18-β-glycyrrhetic acid by nanodelivery systems increases cytotoxicity on oral carcinoma cell line. Nanotechnology 29(28):285101

14.	Sasikanth K, Nama S, Suresh S, Brahmaiah B (2013) Nanofibers-a new trend in nano drug delivery systems. Pharm Innov 2(2):118

15.	Safaeijavan R, Soleimani M, Divsalar A, Eidi A, Ardeshirylajimi A (2014) Biological behavior study of gelatin coated PCL nanofiberous electrospun scaffolds using fibroblasts. Arch Adv Biosci 5(1):562

16.	Beachley V, Wen X (2010) Polymer nanofibrous structures: Fabrication, biofunctionalization, and cell interactions. Progr Polym Sci 35(7):868–892

17.	Chen H, Huang J, Yu J, Liu S, Gu P (2011) Electrospun chitosan-graft-poly (ε-caprolactone)/poly (ε-caprolactone) cationic nanofibrous mats as potential scaffolds for skin tissue engineering. Int J Biol Macromol 48(1):13–19

18.	Ekram B, Abd El-Hady BM, El-Kady AM, Amr SM, Gabr H, Waly AI, Guirguis OW (2019) Enhancing the stability, hydrophilicity, mechanical and biological properties of electrospun poly-caprolactone in formic acid/acetic acid solvent system. Fibers Polym 20:715–724

19.	Ekram B, Abdel-Hady BM, El-kady AM, Amr SM, Waley AI, Guirguis OW (2017) Optimum parameters for the production of nano-scale electrospun polycaprolactone to be used as a biomedical material. Adv Nat Sci Nanosci Nanotechnol 8(4):045018

20.	Kaviannasab E, Semnani D, Khorasani SN, Varshosaz J, Khalili S, Ghahreman F (2019) Core-shell nanofibers of poly (ε–caprolactone) and Polyvinylpyrrolidone for drug delivery system. Mater Res Exp 6(11):115015

21.	Raizada A, Bandari A, Kumar BJIJPRD (2010) Polymers in drug delivery: A review. 2:9–20

22.	Amin A, Samy M, Abd El-Alim SH, Rabia AEG, Ayoub MM (2018) Assessment of formulation parameters needed for successful vitamin C entrapped polycaprolactone nanoparticles. Int J Polym Mater Polym Biomater 67(16):942–950

23.	Nadim A, Khorasani SN, Kharaziha M, Davoodi SM (2017) Design and characterization of dexamethasone-loaded poly (glycerol sebacate)-poly caprolactone/gelatin scaffold by coaxial electro spinning for soft tissue engineering. Mater Sci Eng C 78:47–58

24.	Naeimirad M, Zadhoush A, Kotek R, EsmaeelyNeisiany R, Nouri Khorasani S, Ramakrishna S (2018) Recent advances in core/shell bicomponent fibers and nanofibers: a review. J Appl Polym Sci 135(21):46265

25.	Xu T, Jin W, Wang Z, Cheng H, Huang X, Guo X, Yang H (2018) Electrospun CuO-nanoparticles-modified polycaprolactone@ polypyrrole fibers: an application to sensing glucose in saliva. Nanomaterials 8(3):133

26. Liverani L, Boccaccini AR (2016) Versatile production of poly (epsilon-caprolactone) fibers by electrospinning using benign solvents. Nanomaterials 6(4):75

27. Pal P, Srivas PK, Dadhich P, Das B, Maulik D, Dhara S (2017) Nano-/microfibrous cotton-wool-like 3D scaffold with core–shell architecture by emulsion electrospinning for skin tissue regeneration. ACS Biomater Sci Eng 3(12):3563–3575

28. Bosworth LA, Downes S (2010) Physicochemical characterisation of degrading polycaprolactone scaffolds. Polym Degrad Stab 95(12):2269–2276

29. Kim G, Park J, Park S (2007) Surface-treated and multilayered poly (ε-caprolactone) nanofiber webs exhibiting enhanced hydrophilicity. J Polym Sci Part B Polym Phys 45(15):2038–2045

30. Xu F, Cui FZ, Jiao YP, Meng QY, Wang XP, Cui XY (2009) Improvement of cytocompatibility of electrospinning PLLA microfibers by blending PVP. J Mater Sci Mater Med 20:1331–1338

31. Aldana AA, Malatto L, Rehman MAU, Boccaccini AR, Abraham GA (2019) Fabrication of gelatin methacrylate (GelMA) scaffolds with nano-and micro-topographical and morphological features. Nanomaterials 9(1):120

32. Fallah M, Bahrami SH, Ranjbar-Mohammadi M (2016) Fabrication and characterization of PCL/gelatin/curcumin nanofibers and their antibacterial properties. J Indust Text 46(2):562–577

33. Blackstone BN, Hahn JM, McFarland KL, DeBruler DM, Supp DM, Powell HM (2018) Inflammatory response and biomechanical properties of coaxial scaffolds for engineered skin in vitro and post-grafting. Acta Biomater 80:247–257

34. Zamora-Mora V, Fernández-Gutiérrez M, González-Gómez Á, Sanz B, Román JS, Goya GF et al (2017) Chitosan nanoparticles for combined drug delivery and magnetic hyperthermia: from preparation to in vitro studies. Carbohydr Polym 157:361–370

35. Salar RK, Kumar N (2016) Synthesis and characterization of vincristine loaded folic acid–chitosan conjugated nanoparticles. Resource-Efficient Technol 2:199–214

36. Badran MM, Mady MM, Ghannam MM, Shakeel F (2017) Preparation and characterization of polymeric nanoparticles surface modified with chitosan for target treatment of colorectal cancer. Int J Biol Macromol 95:643–649

37. Kim MS, Jun I, Shin YM, Jang W, Kim SI, Shin H (2010) The development of genipin-crosslinked poly (caprolactone)(PCL)/gelatin nanofibers for tissue engineering applications. Macromol Biosci 10(1):91–100

38. Ramalingam R, Dhand C, Leung CM, Ezhilarasu H, Prasannan P, Ong ST, Arunachalam KD (2019) Poly-ε-caprolactone/gelatin hybrid electrospun composite nanofibrous mats containing ultrasound assisted herbal extract: antimicrobial and cell proliferation study. Nanomaterials 9(3):462

39. Zhang H, Wang Y, Vasilescu S, Gu Z, Sun T (2017) Bio-inspired enhancement of friction and adhesion at the polydimethylsiloxane-intestine interface and biocompatibility characterization. Mater Sci Eng C 74:246–252

40. Iqbal S, Rashid MH, Arbab AS, Khan M (2017) Encapsulation of anticancer drugs (5-fluorouracil and paclitaxel) into polycaprolactone (PCL) nanofibers and in vitro testing for sustained and targeted therapy. J Biomed Nanotechnol 13(4):355–366

41. Nagarwal RC, Kumar R, Pandit J (2012) Chitosan coated sodium alginate–chitosan nanoparticles loaded with 5-FU for ocular delivery: in vitro characterization and in vivo study in rabbit eye. Eur J Pharm Sci 47:678–685

42. Chong LH, Lim MM, Sultana N (2015) Fabrication and evaluation of polycaprolactone/gelatin-based electrospun nanofibers with antibacterial properties. J Nanomater 2015:15–15

43. Ghasemi-Mobarakeh L, Prabhakaran MP, Morshed M, Nasr-Esfahani MH, Ramakrishna S (2008) Electrospun poly (ε-caprolactone)/gelatin nanofibrous scaffolds for nerve tissue engineering. Biomaterials 29(34):4532–4539

44. Gautam S, Dinda AK, Mishra NC (2013) Fabrication and characterization of PCL/gelatin composite nanofibrous scaffold for tissue engineering applications by electrospinning method. Mater Sci Eng C 33(3):1228–1235

45. Samy M, Abdallah HM, Ayoub MM, Vylegzhanina ME, Volkov AY, Sukhanova TE (2020) Eco-friendly route for encapsulation of 5-fluorouracil into polycaprolactone nanoparticles. Egypt J Chem 63(1):255–267

46. Ghahreman F, Semnani D, Khorasani SN, Varshosaz J, Khalili S, Mohammadi S, Kaviannasab E (2020) Polycaprolactone-gelatin membranes in controlled drug delivery of 5-fluorouracil. Polym Sci Ser A 62:636–647

47. Yousefi SR, Ghanbari M, Amiri O, Marzhoseyni Z, Mehdizadeh P, Hajizadeh-Oghaz M et al (2021) $Dy_2BaCuO_5/Ba_4DyCu_3O_9$. 09 S-scheme heterojunction nanocomposite with enhanced photocatalytic and antibacterial activities. J Am Ceram Soc 104:2952–65

48. Kim HW, Knowles JC, Kim HE (2005) The Japanese Society for Biomaterials, Biomaterials TASf, Biomaterials tKSf. Porous scaffolds of gelatin–hydroxyapatite nanocomposites obtained by biomimetic approach: characterization and antibiotic drug release. 74:686–98.

49. Samy M, Abdallah HM, Awad HM, Ayoub MM (2022) In vitro release and cytotoxicity activity of 5-fluorouracil entrapped polycaprolactone nanoparticles. Polym Bull 24:1–27

50. Martins-Franchetti SM, Egerton TA, White JR (2010) Morphological changes in poly (caprolactone)/poly (vinyl chloride) blends caused by biodegradation. J Polym Environ 18:79–83

51. Samy M, Abdallah HM, Awad HM, Ayoub MM (2023) Preparation, characterization and in vitro biological activity of 5-fluorouracil loaded onto poly (D, L-lactic-co-glycolic acid) nanoparticles. Polym Bull 80(6):6197–6219

52. El Fawal G, Hong H, Mo X, Wang H (2021) Fabrication of scaffold based on gelatin and polycaprolactone (PCL) for wound dressing application. J Drug Deliv Sci Technol 63:102501

53. Figueroa-Lopez KJ, Castro-Mayorga JL, Andrade-Mahecha MM, Cabedo L, Lagaron JMJN (2018) Antibacterial and barrier properties of gelatin coated by electrospun polycaprolactone ultrathin fibers containing black pepper oleoresin of interest in active food biopackaging applications. Nanomaterials 8:199

54. Mohamed A, Finkenstadt V, Gordon SH, Biresaw G, Palmquist DE, Rayas-Duarte PJJ (2008) Thermal properties of PCL/gluten bioblends characterized by TGA, DSC, SEM, and infrared-PAS. 110:3256–3266

55. Unal S, Arslan S, Yilmaz BK, Oktar FN, Ficai D, Ficai A et al (2020) Polycaprolactone/gelatin/hyaluronic acid electrospun scaffolds to mimic glioblastoma extracellular matrix. Materials 13:2661

56. Chong LH, Lim MM, Sultana N (2015) Fabrication and evaluation of polycaprolactone/gelatin-based electrospun nanofibers with antibacterial properties. J Nanomater 2015:15

57. Samy M, Abd El-Alim SH, Amin A, Ayoub MMJ (2020) Formulation, characterization and in vitro release study of 5-fluorouracil loaded chitosan nanoparticles. Int J Biol Macromol 156:783–91

58. Kumar SU, Matai I, Dubey P, Bhushan B, Sachdev A, Gopinath PJRA (2014) Differentially cross-linkable core–shell nanofibers for tunable delivery of anticancer drugs: synthesis, characterization and their anticancer efficacy. RSC Adv 4:38263–72

59. Zeng J, Aigner A, Czubayko F, Kissel T, Wendorff JH, Greiner AJB (2005) Poly (vinyl alcohol) nanofibers by electrospinning as a protein delivery system and the retardation of enzyme release by additional polymer coatings. Biomacromoleocules 6:1484–8

60. Kenawy E-R, Abdel-Hay FI, El-Newehy MH, Wnek GE (2009) Processing of polymer nanofibers through electrospinning as drug delivery systems. Nanomater Risks Benefits Springer 8:247–63